Spectroscopy on polymer-fullerene composites and photovoltaic cells

Dyakonov, V.; Godovsky, D.; Parisi, J.; Brabec, C.J.; Sariciftci, N.S.; Hummelen, J.C.; De Ceuster, J.; Goovaerts, E.

Published in:
Synthetic Metals

DOI:
10.1016/S0379-6779(00)01156-5

Publication date:
2001

ELSEVIER

Synthetic Metals 121 (2001) 1529–1532

SYNTHETIC METALS

www.elsevier.com/locate/synmet

Spectroscopy on polymer-fullerene composites and photovoltaic cells

V. Dyakonov [a*], D. Godovsky [a], J. Parisi [a], C. J. Brabec [b], N. S. Sariciftci [b], J. C. Hummelen [c], J. De Ceuster [d], E. Goovaerts [d]

[a] *Department of Energy and Semiconductor Research, University of Oldenburg, 26111 Oldenburg, Germany*
[b] *Christian Doppler Laboratory for Plastic Solar Cells, Johannes Kepler University of Linz, 4040 Linz, Austria*
[c] *Stratingh Institute and Materials Science Center, University of Groningen, Nijenborgh 4, 9747 AG Groningen, The Netherlands*
[d] *Department of Physics, University of Antwerp, 2020 Antwerp, Belgium*

Abstract

We investigate the electrical transport properties of ITO/conjugated polymer-fullerene/Al photovoltaic cells and the role of defect states with the help of admittance spectroscopy and magnetic resonance technique. In the temperature range 293-40K, a characteristic step in the admittance spectrum can be observed originating from the electrically active acceptor level. The activation energy determined from an Arrhenius plot is 34meV. The diode capacitance as a function of the reverse bias is different from the Schottky diode behaviour. We found a bias independent capacitance under reverse bias. This indicates that the devices are either fully depleted, or the space charge region exceeds the device thickness. An efficient generation of charge carriers and their fate in these systems have been studied by electron spin resonance (ESR). We can clearly follow the formation of photo-generated electron-hole pairs under illumination of the device absorber. Using high-frequency (95 GHz) light induced ESR it was possible to separate these two contributions to the spectrum on the basis of their g-parameters, and to resolve the g-anisotropy of the radicals. The P^+-polaron possesses an axial symmetry whereas for C_{60}^- a lower, rhombic symmetry was observed. Important for the cell performance is that photo-generated electron-hole pairs remain in the composites even after the photo-excitation has been switched off, implying the presence of defect-induced trap states.

Keywords: Solar cells, Capacitance, Electron spin resonance, Poly(phenylene-vinylene), Fullerenes and derivatives

1. Introduction

The overall interest in organic donor-acceptor composites grows due to their use in active layers of photovoltaic devices. Photo-induced electron transfer in such composites is a recently discovered phenomenon, the photovoltaic action of the electronic devices is based on [1]. The formation of interpenetrating networks between conjugated polymers and fullerenes is an effective method to increase the charge generating interface in photovoltaic devices and has been successfully utilised in highly efficient plastic solar cells with an energy conversion efficiency of $\eta_e > 1$.

The charge transfer occurs within the sub-picosecond range and the separated state is metastable. The latter may be described as ultrafast formation of pairs of $(D^+ \ldots A^-)$ - type which have a high rate of dissociation and a low rate of recombination. In spite of a high spectral quantum yield of photo-generated charge carriers, the power efficiency is moderate.

Detailed electrical characterisation of these devices provides a deeper understanding of the material properties and the device physics.

2. Experimental

Electrical spectroscopy performed by techniques such as admittance spectroscopy can contribute to the understanding of electric transport processes in the polymer solar cells. The presence of the gap states as well as the interface states may influence the electrical parameters of the cell due to charge carrier trapping. We have studied the admittance and capacitance-voltage (C-V) behaviour of the ITO/MDMO-PPV:PCBM/Al (MDMO-PPV - [poly (2-methoxy-5-(3-,7-dimethyloctyloxy)-1,4-pheny-lene viny-

* Corresponding author. Tel: +49-441-7893538; fax: +49-441-798-3326;
E-mail: dyakonov@uni-oldenburg.de

PII: S0379-6779(00)01556-5

lene]–conjugated polymer, PCBM – [6,6]-phenyl-C_{61}-butyric acid methyl ester - soluble derivative of C_{60}) structures. The cells of 15×15 mm^2 size were fabricated by spin-coating of the polymer-fullerene p-Xylene solution (1:3 weight ratio) on top of a patterned ITO contact on a glass substrate (Scheme 1). We distinguish between Cell 1 (V_{sc}=700mV, J_{sc}=1.49mA/cm^2, FF=0.29, η_e=0.3%) and Cell 2 (V_{sc}=750mV, J_{sc}=5mA/cm^2, FF=0.5, η_e=2.5%). The Cell 1 shows a low rectification (~5) under illumination, in contrast with the Cell 2 (~100).

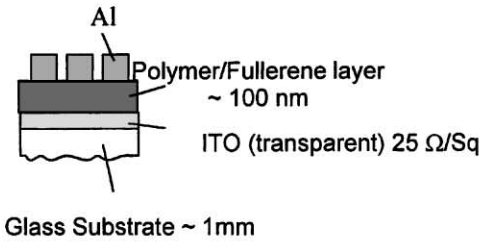

Scheme 1: Device configuration.

Admittance measurements in the range 0.1Hz –10MHz have been performed with a Solartron impedance analyzer 1260A equipped with a Solartron dielectric interface 1296A in combination with a variable temperature helium cryostat (T=40K-320K). The measurements were carried out at oscillator levels below 50mV without dc voltage, in order to work close to equilibrium which can be distorted at high injection of charge carriers. Electron spin resonance (ESR) measurements were performed with a Bruker X-Band (9.5GHz) and W-Band (95GHz) spectrometer in combination with a variable temperature cryostat. For light

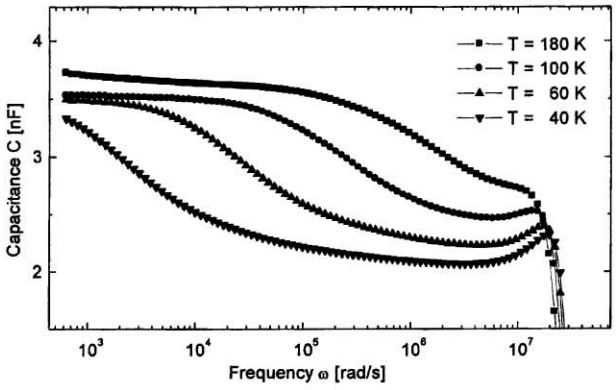

Fig. 1Capacitance vs. frequency of a ITO/MDMO-PPV:PCBM/Al device (Cell 1).

induced ESR studies the samples were illuminated with the 488 nm (≈ 2.5 eV) line of an Ar^+ laser.

3. Experimental Results and Discussion

3.1. Admittance spectroscopy

The frequency dependent contribution to the complex admittance, Y=G+iωC, can originate from the trap levels located in the bulk of the semiconductor material or at the interface. The presence of such states can be seen in the

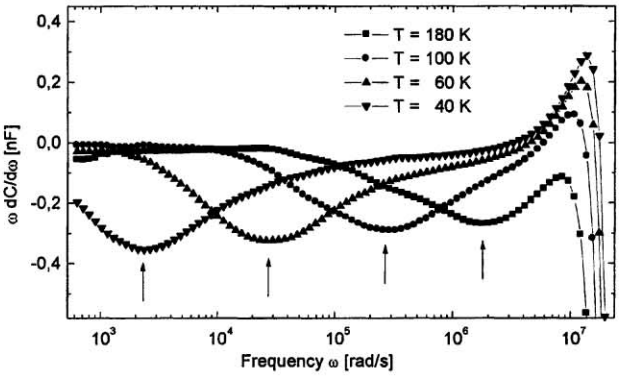

Fig. 2 Differential capacitance vs. frequency of a ITO/MDMO-PPV:PCBM/Al cell (#2).

C(ω) dependence (ω=2πν- angular frequency), where the characteristic steps are expected. Figure 1 shows the C(ω) response of an ITO/MDMO-PPV:PCBM/Al device (Cell 1) at different temperatures. One step can be clearly seen. In the differentiated capacitance spectrum (Figure 2), this step appears as a minimum, which enables to reveal the position

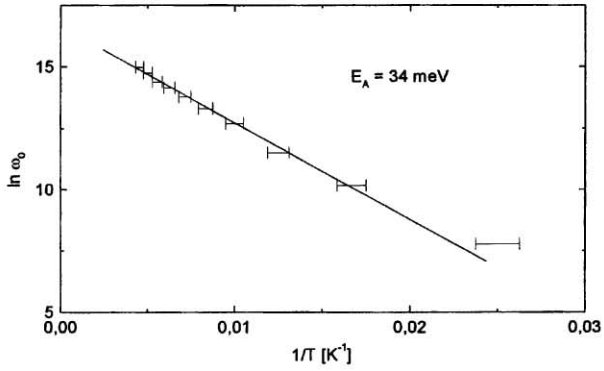

Fig. 3 Frequency minima derived from Fig. 2, and follow the $\ln(\omega_0) \sim -E_A/k \cdot 1/T$).

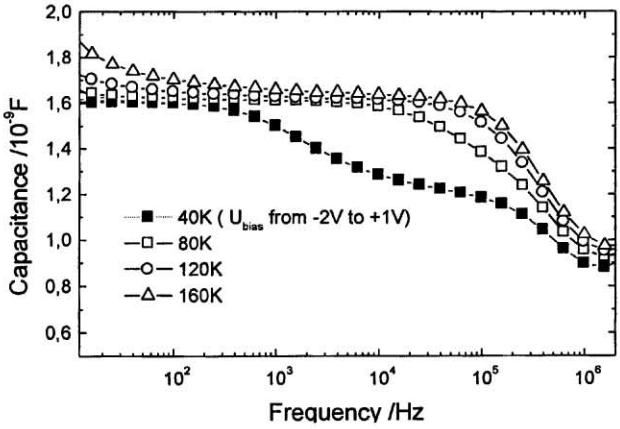

Fig. 4 Capacitance *vs.* frequency at different temperatures and dc bias in Cell 2.

of the step on the frequency axis more accurately. The position of the step does not depend on the bias applied, however, the step shifts to lower frequencies when cooling

down the device from 300K to 40K. The latter is indicative for a thermally activated process with an activation energy E_A= 24-34meV corresponding to a shallow trap level (Fig

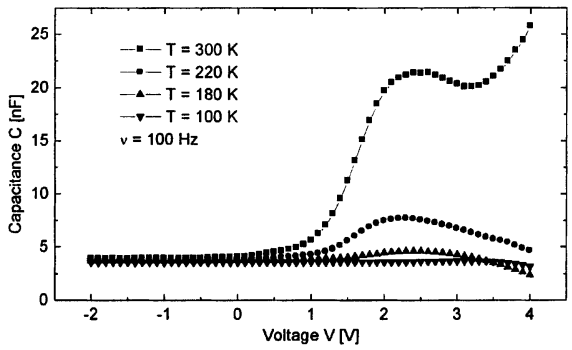

Fig. 5 C-V dependence of the Cell 2 at frequency 100Hz.

3). The C(ω, T) behavior in the high efficiency cells is essentially the same. The same step is observed showing similar values of the thermal activation energy. The capacitance decreases with increasing frequency. Under applied bias from –2V to +2V (T=40K) , the position of the step does not shift along the frequency axis (see Figure 4).

3.2. C-V Measurements

We carried out C-V measurements, to reveal the presence of a space charge region, as a further contribution to the device capacitance. Figure 5 demonstrates the C-V behavior. We found a nearly bias independent capacitance under reverse bias in the low efficiency cell (#1). This indicates that the device is fully depleted. Surprisingly, the capacitance increases and shows a peak at forward bias. Although, we do not have a conclusive model to explain the appearance of the capacitance peak and even a further increase of the capacitance under charge injection conditions, the possible reason can be a charge accumulation layer at the metal/polymer and/or the metal/fullerene interfaces [5], or polymer/fullerene defects. The C-V dependencies of the Cell 2 slightly differ from the ones, observed for Cell 1, mainly in the frequency range above 10 kHz, but the general conclusion on the absence of the space charge region is valid.

4. Electron spin resonance

Electron Spin Resonance is a proven technique for the investigation of radical formation. LESR is well suited for studies of the radical formation under the influence of the light. LESR measurements on composites of conjugated polymers and fullerenes were already performed in a conventional X-band (9.5 GHz) spectrometer [6]. The most important findings were the creation of two radicals: the positive polaron P^+ on the polymer and the C_{60}^- anion radical on the fullerene. We found that signals demonstrate different saturation behavior which is due to different spin lattice relaxation times for photo-generated species. This is

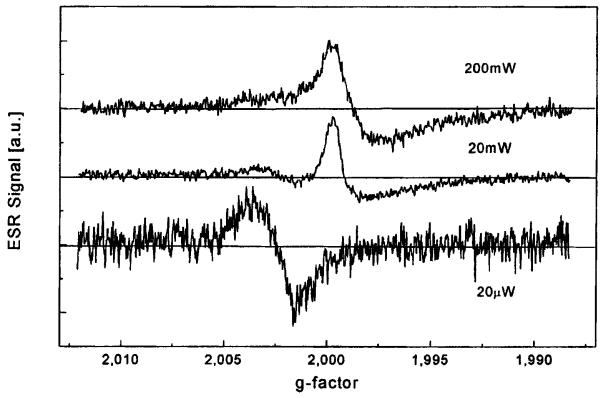

Fig. 6 X-Band (9.5GHz) LESR on a MDMO-PPV/PCBM film at three values of microwave power.

an evidence of the completely independent photo-induced spins without detectable spin-exchange-type correlation effects. Figure 6 shows ESR spectra for three different microwave power values, clearly demonstrating the presence of two signals at different values of the g-factor (g=hν/B, ν- microwave frequency, μ_B – Bohr magneton, B-static magnetic field). We determined the individual g-factors as g=2.0025 and g=1.9995 from the spectrum.

High-Frequency (HF-) LESR can lead to a better understanding of the physics on the molecular scale. On the one hand, HF-LESR can better distinguish between both contributions to the LESR spectrum which are only slightly separated in the g-value in the X-band. Also it is possible to resolve small g-anisotropies of each of the features. In contrast with the X-band LESR, well separated spectral features can be observed in the W-band measurements. As shown in Fig. 7, these features are attributed to the positive polaron P^+ (labeled by $g_\perp$ and $g_{//}$) and the C_{60}^- radical (labeled by g_x, g_y and g_z). Furthermore, HF-LESR resolves

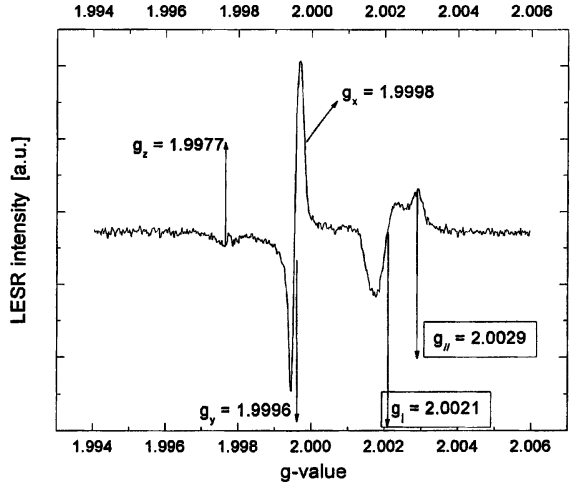

Fig. 7 The W-Band (95GHz) LESR spectrum of the MDMO-PPV/PCBM composite. The small ESR line around g = 1.9977, superimposed onto the g_z of the C_{60}^- is from the reference Mn^{2+}.

the g-anisotropy of both features, revealing the symmetry of the radicals. The axial symmetry of the P^+ is consistent with the localised character of the polaron on the conjugated segment of the PPV chain.

When the excitation light is switched off, the intensity of the X-LESR signals in conjugated polymer/fullerene composites decreases significantly, but not completely. Therefore, we distinguish between the prompt component of LESR, which disappears after the light is off and the persistent component which remains for hours at low temperatures after the illumination is off. Prompt components of the LESR signals which are the difference between spectra with light on and light off, is plotted in Figure 8 as a function of the intensity of the excitation light. It shows an almost equal amount of spins (indicated by double integrated ESR intensities) and I^{α}, α=0.5, a power dependence on the intensity of the excitation light for both LESR signals. The persistent component is nearly independent on the intensity of previously applied light and proposed to originate from deep traps due to disorder.

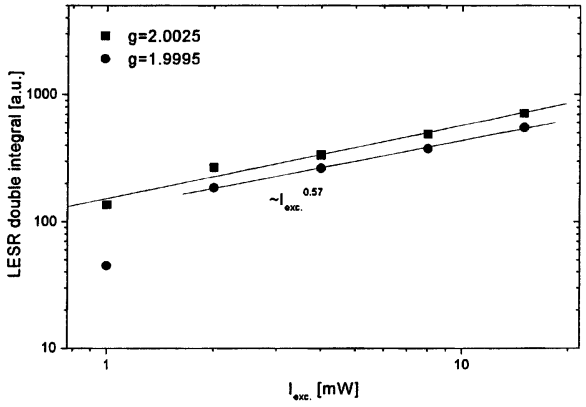

Fig. 8 Dependencies of magnitude of the prompt LESR contributions of the MDMO-PPV/PCBM composite on the intensity of the exciting light.

5. Discussion

The full set of experimental data allows us to conclude that the electrically active defect states, which we observe in the C(ω) dependencies, are situated at the metal/polymer-composite interface. The bias independent position of the step is an evidence for the Fermi level pinning at the interface due to the high density of the defect states. We ruled out the bulk defects, since the process of bulk defect ionization in conjugated polymers consists in the hopping of a hole from the conjugated segment with an acceptor impurity (compensated state) to the neighboring conjugated segment. Such hopping should be bias dependent due to the effective lowering of the potential barriers in high electric fields (Pool-Frenkel mechanism).

Since the LESR signals in conjugated polymer/fullerene composites originate from a photoinduced electron transfer reaction which creates an equal amount of spins (holes on the polymer chain, electrons on the fullerene molecule), one can expect equal areas under the LESR curves. In any case, the sample should remain charge neutral. We observe nearly equal amounts of prompt LESR spins for the two different signals, as indicated by the double integral value of the ESR signal in Fig. 8. Hence, we may conclude that the two photo-induced charges annihilate each other with a bimolecular dynamics. This is confirmed by the $I^{0.5}$ variation of the LESR intensity with the excitation light power.

6. Conclusions

We have examined the electrical transport properties of novel polymer-fullerene solar cells by means of admittance spectroscopy in the temperature range 40-320K. We detect electrically active shallow acceptor levels with E_A=24-34meV situated, from our point of view, at the metal/polymer-composite interface. The high density of interfacial states leads to the pinning of the Fermi level.

An efficient generation of charge carriers and their fate in these systems have been studied by high frequency electron spin resonance. We can clearly follow the formation of photogenerated radical anion/radical cation pairs under illumination of the device absorber. Using high-frequency LESR it was possible to separate these two contributions to the spectrum on the basis of their g-parameters, and to resolve the g-anisotropy of the radicals. The P^{+}-polaron possesses an axial symmetry whereas for C_{60}^{-} a lower, rhombic symmetry was observed. Important for the cell performance is that photogenerated e-h pairs remain in the composites even after the photoexcitation is off, implying the presence of defect induced trap states.

References

[1] N. S. Sariciftci, L. Smilowitz, A. J. Heeger and F. Wudl, *Science*, 258 (1992) 1474.
[2] G. Yu, J. Gao, J. C. Hummelen, F. Wudl and A. J. Heeger, *Science*, 270 (1995) 1789.
[3] see http://www.ipc.uni-linz.ac.at/plastic/page3.html
[4] C. J. Brabec, Proceedings of 16th European Photovoltaic Solar Energy Conversion Conference, Glasgow, UK, 2000.
[5] I. H. Campbell, D. L. Smith, J. P. Ferrairis, Appl. Phys. Lett. 66 (1995) 3030.
[6] V. Dyakonov, G. Zoriniants, M. Scharber, C. J. Brabec, R. A. J. Janssen, J. C. Hummelen, N. S. Sariciftci, Phys. Rev. B 59 (1999) 8019.